Editors' Suggestion

Null tests from angular distributions in $D \to P_1P_2l^+l^-$, $l = e, \mu$ decays on and off peak

Stefan de Boer[1,*] and Gudrun Hiller[2,†]

[1]Institut für Theoretische Teilchenphysik, Karlsruher Institut für Technologie, D-76128 Karlsruhe, Germany

[2]Fakultät Physik, TU Dortmund, Otto-Hahn-Straße 4, D-44221 Dortmund, Germany

(Received 25 May 2018; published 28 August 2018)

We systematically analyze the full angular distribution in $D \to P_1P_2l^+l^-$ decays, where $P_{1,2} = \pi, K$, $l = e, \mu$. We identify several null tests of the standard model (SM). Notably, the angular coefficients $I_{5,6,7}$, driven by the leptons' axial-vector coupling $C_{10}^{(\prime)}$, vanish by means of a superior Glashow-Iliopoulos-Maiani (GIM) cancellation and are protected by parity invariance below the weak scale. CP-odd observables related to the angular coefficients $I_{5,6,8,9}$ allow us to measure CP asymmetries without D tagging. The corresponding observables $A_{5,6,8,9}$ constitute null tests of the SM. Lepton universality in $|\Delta c| = |\Delta u| = 1$ transitions can be tested by comparing $D \to P_1P_2\mu^+\mu^-$ to $D \to P_1P_2e^+e^-$ decays. Data for $P_1P_2 = \pi^+\pi^-$ and K^+K^- on muon modes are available from LHCb and on electron modes from BESIII. Corresponding ratios of dimuon to dielectron branching fractions are at least about an order of magnitude away from probing the SM. In the future electron and muon measurements should be made available for the same cuts as corresponding ratios $R^D_{P_1P_2}$ provide null tests of e-μ universality. We work out beyond-SM signals model-independently and in SM extensions with leptoquarks.

DOI: 10.1103/PhysRevD.98.035041

I. INTRODUCTION

Rare charm decays are notoriously challenging theoretically, yet offer singular insights into flavor in the up-quark sector [1]. With standard model (SM) branching ratios of $|\Delta c| = |\Delta u| = 1$ modes in the 10^{-7}–10^{-6} (semileptonic) and 10^{-6}–10^{-4} (radiative) range, precision studies are feasible at the experiments LHCb [2], Belle II [3] and BESIII [4]. In view of the substantial hadronic uncertainties there are three main avenues to probe for beyond the standard model (BSM) physics in charm: (i) a measurement in an obvious excess of the SM such as the $D \to \pi\mu^+\mu^-$ branching ratio at high dilepton mass [5]—a window that can be closing soon [6], (ii) extract the SM contribution from a SM-dominated mode and use $SU(3)_F$, e.g., recently demonstrated for $D \to V\gamma$, $V = \rho, \bar{K}^*, \phi$ and $D_{(s)} \to K\pi\pi\gamma$ decays in [7] or (iii) perform null tests of (approximate) symmetries of the SM. The latter includes searches for lepton-flavor violation (LFV), CP violation, or lepton nonuniversality (LNU).

In this work we consider angular observables, and LNU tests in semileptonic rare charm decays into electrons and muons. Exclusive semileptonic 3-body charm decays have been studied in some detail in the decays $D \to \pi l^+l^-$ [6,8] and $D \to \rho l^+l^-$ [1,8,9] within QCD factorization (QCDF) [10]. Previous theory works on the four-body decays $D \to P_1P_2l^+l^-$, $P_{1,2} = \pi, K$ highlight T-odd asymmetries [11,12] or the leptonic forward-backward asymmetry [12], however, a systematic analysis of the virtues of the full angular distribution at par with the corresponding one in B decays [13] is missing. Modes sensitive to BSM physics in semileptonic transitions are

$$\begin{aligned} &D^0 \to \pi^+\pi^-l^+l^-, \quad D^0 \to K^+K^-l^+l^-, \\ &\qquad\qquad\qquad\quad D^+ \to K^+\bar{K}^0l^+l^-, \\ &D_s \to K^+\pi^0l^+l^-, \quad D_s \to K^0\pi^+l^+l^-, \end{aligned} \tag{1}$$

which all are singly Cabibbo suppressed. We do not consider $D \to \pi^+\pi^0ll$ decays because isospin-conserving BSM contributions, such as those we are interested in this work, drop out in the isospin limit. However, this mode can complement SM tests in hadronic 2-body decays of charm [11,14–16]. Experimental results on four-body decays exist from LHCb for branching ratios [17] of D^0 decays into

*stefan.boer@kit.edu
†ghiller@physik.uni-dortmund.de

muons and from BESIII for upper limits on branching ratios [18] of D^0, D^+ decays into electrons.

The aim of this work is to study the angular distribution in $D \to P_1 P_2 l^+ l^-$ decays on and off resonance, and to work out opportunities for BSM signals. Related distributions in $B \to K\pi l^+ l^-$ decays have been analyzed in [13]. We describe nonresonant contributions with an operator product expansion (OPE) in $1/Q$, $Q = \{\sqrt{q^2}, m_c\}$, applicable at $q^2 = \mathcal{O}(m_c^2)$ and detailed for $B \to V l^+ l^-$ decays in [19]. Here, q^2 denotes the dilepton invariant mass squared, and m_c is the charm mass. $D \to P_1 P_2$ form factors are available from heavy hadron chiral perturbation theory (HHχPT) [20]. To capture the phenomenology we model resonance effects, which dominate the decay rates, assuming factorization and vector meson dominance, as in [12], amended by data [17].

Despite the significant hadronic uncertainties there are features in the SM which are sufficiently clean to warrant phenomenological exploitation of semileptonic rare charm decays: negligible contributions to axial-vector lepton coupling, $C_{10}^{(\prime)}$, and the suppression of CP, lepton flavor and lepton universality violation. Our proposal to test the SM with $D \to P_1 P_2 l^+ l^-$ decays is based on these features, which allow us to perform null tests and to identify new physics. An interpretation in terms of BSM couplings, however, will again be subject to hadronic uncertainties.

This paper is organized as follows: In Sec. II we review the weak Lagrangian, SM values and constraints on $|\Delta c| = |\Delta u| = 1$ couplings. The $D \to P_1 P_2 l^+ l^-$ angular distribution is given in Sec. III. Phenomenological resonance contributions are discussed in Sec. IV. BSM signals are worked out in Sec. V, where we also discuss LNU-sensitive observables, probing BSM interactions which distinguish between electrons and muons. In Sec. VI we conclude. Auxiliary information on $D \to P_1 P_2 l^+ l^-$ matrix elements is given in the Appendix.

II. WEAK LAGRANGIAN

We consider BSM effects in the semileptonic operators,

$$Q_9 = (\bar{u}\gamma_\mu P_L c)(\bar{l}\gamma^\mu l), \qquad Q_9' = (\bar{u}\gamma_\mu P_R c)(\bar{l}\gamma^\mu l), \tag{2}$$

$$Q_{10} = (\bar{u}\gamma_\mu P_L c)(\bar{l}\gamma^\mu\gamma_5 l), \quad Q_{10}' = (\bar{u}\gamma_\mu P_R c)(\bar{l}\gamma^\mu\gamma_5 l), \tag{3}$$

$$Q_S = (\bar{u}P_R c)(\bar{l}l), \qquad Q_S' = (\bar{u}P_L c)(\bar{l}l), \tag{4}$$

$$Q_P = (\bar{u}P_R c)(\bar{l}\gamma_5 l), \qquad Q_P' = (\bar{u}P_L c)(\bar{l}\gamma_5 l), \tag{5}$$

$$Q_T = \frac{1}{2}(\bar{u}\sigma^{\mu\nu} c)(\bar{l}\sigma_{\mu\nu} l), \qquad Q_{T5} = \frac{1}{2}(\bar{u}\sigma^{\mu\nu} c)(\bar{l}\sigma_{\mu\nu}\gamma_5 l), \tag{6}$$

in the effective Lagrangian

$$\mathcal{L}_{\rm eff}^{\rm weak} = \frac{4G_F}{\sqrt{2}}\frac{\alpha_e}{4\pi}\Bigg(\sum_{q=d,s} V_{cq}^* V_{uq} \sum_{i=1}^{2} C_i Q_i^{(q)} + \sum_{i=9,10,S,P} (C_i Q_i + C_i' Q_i') + C_T Q_T + C_{T5} Q_{T5}\Bigg), \tag{7}$$

where G_F is the Fermi constant, α_e denotes the fine structure constant and V_{ij} are Cabibbo-Kobayashi-Maskawa (CKM) matrix elements. P_L, P_R denote left- and right-chiral projectors, respectively.

In the SM, the four-quark operators $Q_{1,2}^{(q)} \sim (\bar{u}\gamma_\mu P_L q)(\bar{q}\gamma^\mu P_L c)$ give rise to the dominant contributions to the branching ratios in $|\Delta c| = |\Delta u| = 1$ decays. The Wilson coefficients of the BSM-sensitive operators given in (2)–(6), on the other hand, are subject to an efficient GIM-cancellation, and suppressed. At the charm mass scale $\mu = m_c$ at next-to-next-to-leading-order [6,21,22],

$$|C_7^{\rm eff}| \simeq \mathcal{O}(0.001), \qquad |C_9^{\rm eff}|_{\rm high\,q^2} \lesssim 0.01, \qquad C_{10,S,P,T,T5}^{\rm SM} = 0. \tag{8}$$

Here, the coefficient of the dipole operator $Q_7 = \frac{m_c}{e}(\bar{u}\sigma_{\mu\nu} P_R c) F^{\mu\nu}$, where $F^{\mu\nu}$ denotes the electromagnetic field strength tensor, is also given for completeness. The effective coefficients $C_{7,9}^{\rm eff}$ equal $C_{7,9}$ up to matrix elements of 4-quark operators which relax the GIM cancellation, thus being the dominant contribution [6,22] and inducing a q^2 dependence, see [23].

In addition, all primed coefficients C_i' are negligible in the SM. Experimental constraints, available from the upper limit on the $D^+ \to \pi^+\mu^+\mu^-$ branching ratio, and $D^0 \to \rho^0\gamma$ are presently very weak, at least about 2 orders of magnitude away from the SM [6,24]

$$|C_7^{(\prime)}| \lesssim 0.3, \qquad |C_{9,10}^{(\prime)}| \lesssim 1, \qquad |C_{T,T5}| \lesssim 1, \qquad |C_{S,P}^{(\prime)}| \lesssim 0.1, \tag{9}$$

see [6] for correlated constraints. Corresponding constraints on $c \to u e^+ e^-$ processes are about a factor 2–4 (5 times for C_{T,T_5}) weaker than the ones in (9) on dimuons. Constraints on LFV processes $c \to u e^\pm \mu^\mp$ are 6–7 times (4 times for $C_{S,P}^{(\prime)}$) weaker than the dimuon constraints. To discuss LNU or LFV, Wilson coefficients and operators become lepton-flavor dependent. To avoid clutter, we refrain from showing lepton-flavor superscripts throughout this paper.

III. FULL ANGULAR DISTRIBUTION

In Sec. III A we discuss the full angular distribution for $D \to P_1 P_2 l^+ l^-$ decays and identify SM null tests that exist

thanks to the extreme GIM suppression in charm. In Sec. III B we give the angular distribution in the low hadronic recoil OPE, which defines a factorization-type framework at leading order in $1/m_c$. To estimate possible BSM signals, which involve SM-BSM interference, we need to estimate SM contributions to decay amplitudes as well. The phenomenological description of the dominant resonance-induced contributions is detailed in Sec. IV.

A. General case

The $D \to P_1 P_2 l^+ l^-$ angular distribution, with the angles θ_l, θ_{P_1}, ϕ defined as in [25] taking into account footnote 2 of Ref. [26], can be written as

$$d^5\Gamma = \frac{1}{2\pi}\left[\sum c_i(\theta_l,\phi) I_i(q^2, p^2, \cos\theta_{P_1})\right] \times dq^2 dp^2 d\cos\theta_{P_1} d\cos\theta_l d\phi, \tag{10}$$

where q^2, p^2 denotes the invariant mass squared of the dileptons, (P_1P_2) subsystem, respectively, and

$$\begin{aligned} &c_1 = 1, \qquad c_2 = \cos 2\theta_l, \qquad c_3 = \sin^2\theta_l \cos 2\phi, \\ &c_4 = \sin 2\theta_l \cos\phi, \qquad c_5 = \sin\theta_l \cos\phi, \\ &c_6 = \cos\theta_l, \qquad c_7 = \sin\theta_l \sin\phi, \\ &c_8 = \sin 2\theta_l \sin\phi, \qquad c_9 = \sin^2\theta_l \sin 2\phi. \end{aligned} \tag{11}$$

θ_l denotes the angle between the l^--momentum and the D-momentum in the dilepton center-of-mass system (cms), θ_{P_1} is the angle between the P_1-momentum and the negative direction of flight of the D-meson in the (P_1P_2) cms, and ϕ is the angle between the normals of the (P_1P_2) plane and the (ll) plane in the D rest frame. The angles are within the ranges

$$-1 < \cos\theta_{P_1} \le 1, \quad -1 < \cos\theta_l \le 1, \quad 0 < \phi \le 2\pi. \tag{12}$$

P_1 is the meson that contains the quark emitted from the semileptonic weak $\bar{u}cll$ vertex. For instance, $P_1 = \pi^+$ and $P_1 = K^+$ in the D^0, D^+ decays in (1).

The angular coefficients $I_i \equiv I_i(q^2, p^2, \cos\theta_{P_1})$ are given in terms of transversity amplitudes[1] as

$$\begin{aligned} I_1 &= \frac{1}{16}\left[|H_0^L|^2 + (L\to R) + \frac{3}{2}\sin^2\theta_{P_1}\{|H_\perp^L|^2 + |H_\parallel^L|^2 + (L\to R)\}\right], \\ I_2 &= -\frac{1}{16}\left[|H_0^L|^2 + (L\to R) - \frac{1}{2}\sin^2\theta_{P_1}\{|H_\perp^L|^2 + |H_\parallel^L|^2 + (L\to R)\}\right], \\ I_3 &= \frac{1}{16}[|H_\perp^L|^2 - |H_\parallel^L|^2 + (L\to R)]\sin^2\theta_{P_1}, \\ I_4 &= -\frac{1}{8}[\mathrm{Re}(H_0^L H_\parallel^{L*}) + (L\to R)]\sin\theta_{P_1}, \\ I_5 &= -\frac{1}{4}[\mathrm{Re}(H_0^L H_\perp^{L*}) - (L\to R)]\sin\theta_{P_1}, \\ I_6 &= \frac{1}{4}[\mathrm{Re}(H_\parallel^L H_\perp^{L*}) - (L\to R)]\sin^2\theta_{P_1}, \\ I_7 &= -\frac{1}{4}[\mathrm{Im}(H_0^L H_\parallel^{L*}) - (L\to R)]\sin\theta_{P_1}, \\ I_8 &= -\frac{1}{8}[\mathrm{Im}(H_0^L H_\perp^{L*}) + (L\to R)]\sin\theta_{P_1}, \\ I_9 &= \frac{1}{8}[\mathrm{Im}(H_\parallel^{L*} H_\perp^L) + (L\to R)]\sin^2\theta_{P_1}. \end{aligned} \tag{13}$$

The subscript 0, $\parallel$ and $\perp$ stands for longitudinal, parallel and perpendicular polarization, respectively. Here, L, R denotes the handedness of the lepton current. In the SM electromagnetically induced contributions dominate $c \to u l^+ l^-$ transitions due to the GIM mechanism (8). Hence, by inspecting the relative signs between the left-handed and the right-handed contributions in (13), it follows that $I_{5,6,7}$ constitute null tests, as they require axial-vector contributions to be nonvanishing.

One may wonder about backgrounds to $I_{5,6,7}^{\mathrm{SM}} = 0$. Intermediate pseudoscalar resonances $D \to P_1 P_2 \eta^* \to P_1 P_2 l^+ l^-$ induce a contribution to pseudoscalar operators Q_P not included in (15). The impact can be read off from the $D \to V(\to P_1P_2) l^+ l^-$ angular distribution [26]: Contributions from C_P to $I_{5,6,7}$ require the presence of tensor operators. Similarly, lepton mass effects pose no challenge to the null tests, as finite m_l contributions require the presence of scalar or tensor operators, which are both negligible in the SM (8). Finite SM contributions to axial-vector couplings are expected to arise from higher order electromagnetic effects. For instance, a 2-loop diagram with an insertion of $Q_{1,2}^{(q)}$ with two photons induces a contribution at the relative order $\alpha_e/(4\pi)$, about permille level. We estimate contributions from electromagnetic operator mixing as $C_{10} < 0.01 C_9$ [23,27,28], which is small, at most 10^{-4} in the SM (8). As will be shown in Sec. V A, order one BSM contributions are needed to generate finite angular coefficients up to few percent. Therefore, higher order effects are of no concern to the

[1] No tensor and no (pseudo)-scalar operators included, and for vanishing lepton mass.

null tests $I_{5,6,7}$ within the accuracy that can be achieved in the foreseeable future, 3%(1%) at Run II (upgrade) on $D^0 \to \pi^+\pi^-\mu^+\mu^-$ asymmetries at LHCb [29]. We learn that angular analysis in charm is simpler than in B decays *because* charm is dominated by resonances.

Integrating (10) over ϕ, $\cos\theta_l$ and both, respectively, yields the decay distributions

$$\frac{d^4\Gamma}{dq^2 dp^2 d\cos\theta_{P_1} d\cos\theta_l} = I_1 + I_2\cos 2\theta_l + I_6\cos\theta_l, \tag{14}$$

$$\frac{d^4\Gamma}{dq^2 dp^2 d\cos\theta_{P_1} d\phi} = \frac{1}{\pi}\left(I_1 - \frac{I_2}{3} + \frac{\pi}{4}I_5\cos\phi + \frac{\pi}{4}I_7\sin\phi + \frac{2}{3}I_3\cos 2\phi + \frac{2}{3}I_9\sin 2\phi\right), \tag{15}$$

$$\frac{d^3\Gamma}{dq^2 dp^2 d\cos\theta_{P_1}} = 2\left(I_1 - \frac{I_2}{3}\right). \tag{16}$$

The forward-backward asymmetry in the leptons, $A_{\rm FB} \propto I_6$ can be obtained from asymmetric $\cos\theta_l$ integration

$$I_6 = \frac{1}{2}\left[\int_0^1 d\cos\theta_l - \int_{-1}^0 d\cos\theta_l\right]\frac{d^4\Gamma}{dq^2 dp^2 d\cos\theta_{P_1} d\cos\theta_l}. \tag{17}$$

The observables I_7 and I_5 can be obtained, for instance, as follows:

$$I_7 = \left[\int_0^\pi d\phi - \int_\pi^{2\pi} d\phi\right]\frac{d^4\Gamma}{dq^2 dp^2 d\cos\theta_{P_1} d\phi}, \tag{18}$$

$$I_5 = \left[\int_{-\pi/2}^{\pi/2} d\phi - \int_{\pi/2}^{3\pi/2} d\phi\right]\frac{d^4\Gamma}{dq^2 dp^2 d\cos\theta_{P_1} d\phi}. \tag{19}$$

Methods to get angular coefficients for P-wave contributions are given in [25].

At the kinematic end point of zero hadronic recoil the following exact relations hold [13]:

$$I_3 = -\frac{I_1 + I_2}{2},$$
$$I_4 = -\sqrt{\frac{(I_1 + I_2)(I_1 - 3I_2)}{2}}, \qquad I_{5,6,7,8,9} = 0. \tag{20}$$

The corresponding observables of the CP-conjugated $\bar D$ decays are given by $I_{1,2,3,4,7} \to \bar I_{1,2,3,4,7}$ and $I_{5,6,8,9} \to -\bar I_{5,6,8,9}$, where $\bar I$ equals I with the weak phases flipped. In $\bar D$ decays, θ_l is the angle between the l^--momentum and $\bar D$-momentum in the dilepton cms, θ_{P_1} is the angle between the P_1-momentum and the negative $\bar D$-momentum in the (P_1P_2) cms, and ϕ the angle between the (P_1P_2) and (ll) planes. We keep the definition of P_1 from D decays for $\bar D$ decays.

The observables $I_{7,8,9}$ are (naive) T-odd and corresponding CP asymmetries are not suppressed by small strong phases. The observables $I_{5,6,8,9}$ are odd under the CP transformation. Therefore, if distributions from (untagged) D^0 and $\bar D^0$ decays are averaged one measures a CP asymmetry, A_k, $k = 5, 6, 8, 9$. Due to the smallness of $V_{cb}^* V_{ub}/(V_{cs}^* V_{us})$ these constitute null tests of the SM. Note that time-dependent effects in angular observables [25] are suppressed by the small $D^0 - \bar D^0$ width difference [30].

B. OPE and factorization

At leading order low recoil OPE, long- and short-distance physics factorizes as follows [13]:

$$\begin{aligned}
I_1 &= \frac{1}{8}\left[|\mathcal{F}_0|^2\rho_1^- + \frac{3}{2}\sin^2\theta_{P_1}\{|\mathcal{F}_\parallel|^2\rho_1^- + |\mathcal{F}_\perp|^2\rho_1^+\}\right],\\
I_2 &= -\frac{1}{8}\left[|\mathcal{F}_0|^2\rho_1^- - \frac{1}{2}\sin^2\theta_{P_1}\{|\mathcal{F}_\parallel|^2\rho_1^- + |\mathcal{F}_\perp|^2\rho_1^+\}\right],\\
I_3 &= \frac{1}{8}[|\mathcal{F}_\perp|^2\rho_1^+ - |\mathcal{F}_\parallel|^2\rho_1^-]\sin^2\theta_{P_1},\\
I_4 &= -\frac{1}{4}\mathrm{Re}(\mathcal{F}_0\mathcal{F}_\parallel^*)\rho_1^-\sin\theta_{P_1},\\
I_5 &= [\mathrm{Re}(\mathcal{F}_0\mathcal{F}_\perp^*)\mathrm{Re}\rho_2^+ + \mathrm{Im}(\mathcal{F}_0\mathcal{F}_\perp^*)\mathrm{Im}\rho_2^-]\sin\theta_{P_1},\\
I_6 &= -[\mathrm{Re}(\mathcal{F}_\parallel\mathcal{F}_\perp^*)\mathrm{Re}\rho_2^+ + \mathrm{Im}(\mathcal{F}_\parallel\mathcal{F}_\perp^*)\mathrm{Im}\rho_2^-]\sin^2\theta_{P_1},\\
I_7 &= \mathrm{Im}(\mathcal{F}_0\mathcal{F}_\parallel^*)\delta\rho\sin\theta_{P_1},\\
I_8 &= \frac{1}{2}[\mathrm{Re}(\mathcal{F}_0\mathcal{F}_\perp^*)\mathrm{Im}\rho_2^+ - \mathrm{Im}(\mathcal{F}_0\mathcal{F}_\perp^*)\mathrm{Re}\rho_2^-]\sin\theta_{P_1},\\
I_9 &= \frac{1}{2}[\mathrm{Re}(\mathcal{F}_\perp\mathcal{F}_\parallel^*)\mathrm{Im}\rho_2^+ + \mathrm{Im}(\mathcal{F}_\perp\mathcal{F}_\parallel^*)\mathrm{Re}\rho_2^-]\sin^2\theta_{P_1},
\end{aligned} \tag{21}$$

where the short-distance coefficients read

$$\begin{aligned}
\rho_1^\pm &= |C_9^{\rm eff} \pm C_9'|^2 + |C_{10} \pm C_{10}'|^2,\\
\delta\rho &= \mathrm{Re}[(C_9^{\rm eff} - C_9')(C_{10} - C_{10}')^*],\\
\mathrm{Re}\rho_2^+ &= \mathrm{Re}[C_9^{\rm eff}C_{10}^* - C_9'C_{10}'^*],\\
\mathrm{Im}\rho_2^+ &= \mathrm{Im}[C_{10}'C_{10}^* + C_9'C_9^{\rm eff *}],\\
\mathrm{Re}\rho_2^- &= \frac{1}{2}[|C_{10}|^2 - |C_{10}'|^2 + |C_9^{\rm eff}|^2 - |C_9'|^2],\\
\mathrm{Im}\rho_2^- &= \mathrm{Im}[C_{10}'C_9^{\rm eff *} - C_{10}C_9'^*].
\end{aligned} \tag{22}$$

As we are anticipating BSM contributions to semileptonic operators (2), (3) only[2] we dropped the contributions from

[2]BSM effects in dipole operators can be tested in radiative D decays, e.g., [7,24,31].

dipole operators, which enter as $\propto (m_c m_D/q^2) C_7^{\rm eff}$ for clarity. Full formulas can be seen in [13]. We explicitly checked that contributions from dipole operators are negligible for the purpose of our analysis.

The transversity form factors $\mathcal{F}_i$, $i = 0, \perp, \parallel$ can be written as

$$\begin{aligned}
\mathcal{F}_0 &= \frac{\mathcal{N}_{\rm nr}}{2}\Big[\lambda^{1/2} w_+(q^2, p^2, \cos\theta_{P_1}) \\
&\quad + \frac{1}{p^2}\{(m_{P_1}^2 - m_{P_2}^2)\lambda^{1/2} \\
&\quad - (m_D^2 - q^2 - p^2)\lambda_p^{1/2}\cos\theta_{P_1}\} \\
&\quad \times w_-(q^2, p^2, \cos\theta_{P_1})\Big], \\
\mathcal{F}_\parallel &= \mathcal{N}_{\rm nr}\sqrt{\lambda_p \frac{q^2}{p^2}} w_-(q^2, p^2, \cos\theta_{P_1}), \\
\mathcal{F}_\perp &= \frac{\mathcal{N}_{\rm nr}}{2}\sqrt{\lambda\lambda_p \frac{q^2}{p^2}} h(q^2, p^2, \cos\theta_{P_1}), \\
\mathcal{N}_{\rm nr} &= \frac{G_F \alpha_e}{2^7 \pi^4 m_D}\sqrt{\pi \frac{\sqrt{\lambda\lambda_p}}{m_D p^2}}.
\end{aligned} \tag{23}$$

Here, $\lambda = \lambda(m_D^2, q^2, p^2)$ and $\lambda_p = \lambda(p^2, m_{P_1}^2, m_{P_2}^2)$, where $\lambda(a,b,c) = a^2 + b^2 + c^2 - 2(ab + ac + bc)$. The $D \to P_1 P_2$ transition form factors are defined as

$$\begin{aligned}
&\langle P_1(p_1) P_2(p_2)|\bar{u}\gamma_\mu(1-\gamma_5)c|D(p_D)\rangle \\
&\quad = i[w_+ p_\mu + w_- P_\mu + r q_\mu + i h \epsilon_{\mu\alpha\beta\gamma} p_D^\alpha p^\beta P^\gamma],
\end{aligned} \tag{24}$$

$$\begin{aligned}
&\langle P_1(p_1) P_2(p_2)|\bar{u} i q^\nu \sigma_{\mu\nu}(1+\gamma_5)c|D(p_D)\rangle \\
&\quad = -i m_D[w'_+ p_\mu + w'_- P_\mu + r' q_\mu + i h' \varepsilon_{\mu\alpha\beta\gamma} p_D^\alpha p^\beta P^\gamma],
\end{aligned} \tag{25}$$

where the right-hand sides have to be multiplied by an isospin factor of $1/\sqrt{2}$ for every neutral pion in the final state and we tacitly suppressed the dependence on q^2, p^2 and $\cos\theta_{P_1}$ in the form factors. Here, $q^\mu = p_+^\mu + p_-^\mu$, $p^\mu = p_1^\mu + p_2^\mu = p_D^\mu - q^\mu$ and $P^\mu = p_1^\mu - p_2^\mu$. Since the dipole operators in the SM are negligible and we do not consider BSM tensor operators, the dipole form factors (25) are not needed for our analysis. $r^{(\prime)}$ does not contribute to $D \to P_1 P_2 l^+ l^-$ decays for $m_l = 0$.[3]

The relevant nonresonant $D \to P_1 P_2$ form factors $w_\pm$, h are available from HHχPT [20]. Numerical input is given in the Appendix. Note that HHχPT applies if the participating light mesons are sufficiently soft. We find that $E_\pi - m_\pi$ in the D-meson's cms in $D \to \pi^+\pi^- l^+ l^-$ decays does not exceed 0.4 (0.6) GeV for q^2 above m_ϕ^2 (m_ρ^2), where E_π denotes the energy of any of the pions in the D cms. The region above m_ϕ^2 is kinematically closed for $D \to K^+K^- l^+ l^-$ decays. In these decays $E_K - m_K$ in the D cms does not exceed 0.3 GeV for all q^2, where E_K denotes the energy of any of the kaons in the D cms. Although formally they are limited to low hadronic recoil we use the HHχPT form factors in the full phase space also for $D \to \pi^+\pi^- l^+ l^-$ in absence of other estimates. While this procedure leaves room for improvement, it does not invalidate the null test feature of the observables we discuss as a probe of BSM physics.

We use this prescription, factorization plus HHχPT form factors, for the BSM short-distance contributions from 4-fermion operators (2), (3) to estimate BSM signals in the whole phase space for both $\pi\pi$ and KK modes. In Fig. 1 the q^2, p^2-phase space for $D^0 \to \pi^+\pi^- l^+ l^-$ (plot to the left) and $D^0 \to K^+K^- l^+ l^-$ decays (plot to the right) is shown with dominant resonances. The OPE formally applies for $q^2 = \mathcal{O}(m_c^2)$. This is approximately the region above the ϕ peak in $D \to \pi^+\pi^- l^+ l^-$ decays, and nowhere in $D \to K^+K^- l^+ l^-$. QCDF at least formally works for $p^2 = \mathcal{O}(\Lambda^2)$ and $p^2 \sim q^2$, that is, when the $(P_1 P_2)$ system is light and energetic in the D cms, see also [32]. While QCDF therefore can be used in $D^0 \to \pi^+\pi^- l^+ l^-$ for low q^2, this region is mostly occupied by resonances. In $D \to K^+K^- l^+ l^-$ with $p_{\rm min}^2 \approx 1\ {\rm GeV}^2$ there is little room left. For $p^2 = \mathcal{O}(m_c^2)$ the dilepton system is soft in the D cms. A related discussion of phase space has been given in [33] for $B \to \pi\pi l\nu$ decays. Due to the lower value of the heavy quark mass the phase space in charm is much more compressed than in b decays.

IV. RESONANCE CONTRIBUTIONS

Several resonances contribute to $D \to P_1 P_2 l^+ l^-$ decays. First we consider resonances in the $(P_1 P_2)$ subsystem, that is, in p^2. Depending on the spin $j = 0, 1, \ldots$ of the resonance, such contributions are termed $S, P, \ldots$ wave, respectively. Due to the lower mass of the D-mesons relative to the B ones, there are fewer resonances and ones with lower spin contributing in charm. Lowest lying resonances with sizable branching ratios into $\pi\pi$ are the ρ and scalars $\sigma = f_0(500)$ and $f_0(980)$. At spin 2 there is the $f_2(1270)$. For K^+K^-, it is essentially the ϕ, and for $K\pi$ there is the $K^*(892)$, the scalars κ and $K_0^*(1430)$ and the spin 2 resonance $K_2^*(1430)$.

We model the resonance structure in p^2 for $D^0 \to \pi^+\pi^- l^+ l^-$ decays by the ρ contribution, which is dominant at least in the wider vicinity of $p^2 \approx m_\rho^2$. $D \to \rho$ form factors are taken from [34], see the Appendix. D waves and higher are phase space suppressed relative to the ρ and contribute to small $q^2 \lesssim 0.4\ {\rm GeV}^2$ only. Further study

[3](Pseudo)-scalar operators would also require r, $\langle P_1(p_1) P_2(p_2)|\bar{u}(1+\gamma_5)c|D(p_D)\rangle = i/m_c[w_+ p\cdot q + w_- P\cdot q + r q^2]$.

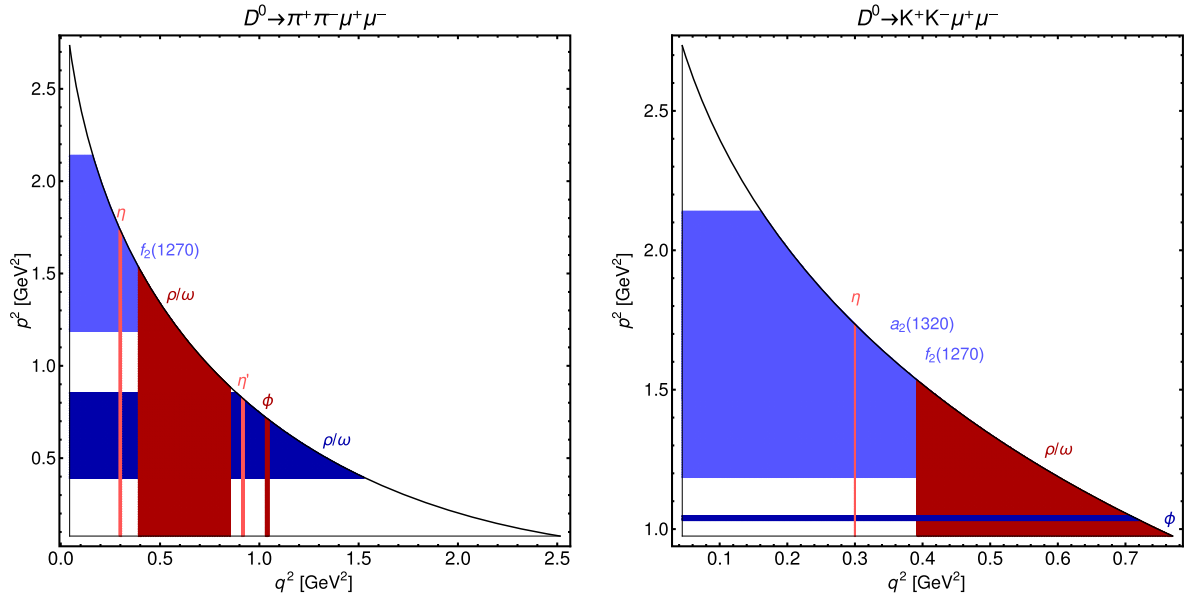

FIG. 1. Phase space and dominant resonances in q^2 and p^2 for $D^0 \to \pi^+\pi^-\mu^+\mu^-$ decays (left) and $D^0 \to K^+K^-\mu^+\mu^-$ decays (right). The bands correspond to (mass $\pm$ width)^2. The very wide scalar resonances $f_0(500)$ and $f_0(980)$ would fill everything below the f_2 in the $\pi\pi$ plot and are not shown.

including scalar contributions, which are rather wide and less known, is beyond the scope of this work, which aims at identifying null tests and illustrating the sensitivity to BSM physics. We stress, however, that since there is no S-wave contribution to $I_{3,6,9}$ [13] these angular coefficients are unaffected by scalars. In addition, the S-P interference terms in $I_{4,5,7,8}$ can be separated from the P-wave contribution by angular analysis, therefore scalars can be experimentally subtracted in these coefficients.

The other type of resonances contribute in q^2 as $D \to P_1P_2\gamma^*$, $\gamma^* \to l^+l^-$ via ω, ρ^0, ϕ and $\eta^{(\prime)}$. We model these contributions with a phenomenological Breit-Wigner shape for $C_9 \to C_9^{\rm R}$ for vector and $C_P \to C_P^{\rm R}$ for pseudoscalar mesons [6,8]

$$C_9^{\rm R} = a_\rho e^{i\delta_\rho}\left(\frac{1}{q^2 - m_\rho^2 + im_\rho\Gamma_\rho} - \frac{1}{3}\frac{1}{q^2 - m_\omega^2 + im_\omega\Gamma_\omega}\right) + \frac{a_\phi e^{i\delta_\phi}}{q^2 - m_\phi^2 + im_\phi\Gamma_\phi},$$
$$C_P^{\rm R} = \frac{a_\eta e^{i\delta_\eta}}{q^2 - m_\eta^2 + im_\eta\Gamma_\eta} + \frac{a_{\eta'}}{q^2 - m_{\eta'}^2 + im_{\eta'}\Gamma_{\eta'}}, \quad (26)$$

where m_M, Γ_M denotes the mass and total width, respectively, of the resonance $M = \eta^{(\prime)}$, ρ^0, ω, ϕ, and we used isospin to relate the ρ^0 to the ω. Corresponding transversity form factors are given in the Appendix, Eqs. (A2)–(A5). LHCb [17] has provided branching ratios in q^2 bins around the resonances ρ/ω and ϕ,

$$\mathcal{B}(D^0 \to \pi^+\pi^-\mu^+\mu^-)|_{[0.565-0.950]\ \rm GeV} = (40.6 \pm 5.7) \times 10^{-8}, \quad (27)$$

$$\mathcal{B}(D^0 \to \pi^+\pi^-\mu^+\mu^-)|_{[0.950-1.100]\ \rm GeV} = (45.4 \pm 5.9) \times 10^{-8}, \quad (28)$$

$$\mathcal{B}(D^0 \to K^+K^-\mu^+\mu^-)|_{[>0.565]\ \rm GeV} = (12.0 \pm 2.7) \times 10^{-8}, \quad (29)$$

where we added uncertainties in quadrature and neglected correlations. The resonance parameters in $C_{9,P}^{\rm R}$ are in general p^2 dependent. We assume that the dominant p^2 dependence is taken care of by the ρ line shape specified in the Appendix such that the a_M are fixed by (27), (28) at $p^2 \approx m_\rho^2$:

$$a_\phi^{\pi\pi} \simeq 0.3\ \text{GeV}^2, \qquad a_\rho^{\pi\pi} \simeq 0.7\ \text{GeV}^2. \quad (30)$$

For $M = \eta^{(\prime)}$ we use $\mathcal{B}(D^0 \to \pi^+\pi^- M(\to \mu^+\mu^-)) \simeq \mathcal{B}(D^0 \to M\pi^+\pi^-)\mathcal{B}(M \to \mu^+\mu^-)$ and take the right-hand side from data [35] together with $\mathcal{B}(\eta' \to \mu^+\mu^-) \sim \mathcal{O}(10^{-7})$ [35,36]. We obtain

$$a_\eta^{\pi\pi} \simeq 0.001\ \text{GeV}^2, \qquad a_{\eta'}^{\pi\pi} \sim 0.001\ \text{GeV}^2. \quad (31)$$

To implement the pseudoscalar contributions we employed the $D \to \rho l^+l^-$ distributions that can be inferred from [26]. We note that fitting $M = \rho^0$, ω, ϕ in the zero-width

TABLE I. Branching ratios for $D^0 \to \pi^+\pi^- l^+ l^-$ and $D^0 \to K^+K^- l^+ l^-$ from data, LHCb [17] ($l = \mu$) and BESIII [18] ($l = e$), our evaluation, resonant and nonresonant, and [12]. Upper limits are at 90% CL.

Branching ratio	$D^0 \to \pi^+\pi^-\mu^+\mu^-$	$D^0 \to K^+K^-\mu^+\mu^-$	$D^0 \to \pi^+\pi^- e^+e^-$	$D^0 \to K^+K^- e^+e^-$
LHCb [17]†	$(9.64 \pm 1.20) \times 10^{-7}$	$(1.54 \pm 0.33) \times 10^{-7}$	⋯	⋯
BESIII [18]	⋯	⋯	$<0.7 \times 10^{-5}$	$<1.1 \times 10^{-5}$
Resonant	$\sim 1 \times 10^{-6}$	$\sim 1 \times 10^{-7}$	$\sim 10^{-6}$	$\sim 10^{-7}$
Nonresonant	10^{-10}–10^{-9}	$\mathcal{O}(10^{-10})$	10^{-10}–10^{-9}	$\mathcal{O}(10^{-10})$
[12]	$\sim 10^{-6}$	$\sim 10^{-7}$	$\sim 10^{-6}$	$\sim 10^{-7}$

†Statistical and systematic uncertainties are added in quadrature.

approximation [35] and using $2 \times \mathcal{B}(D^0 \to \rho^0\rho^0) \times \mathcal{B}(\rho^0 \to \mu^+\mu^-)$ for the ρ^0, one obtains parameters consistent with (30), with a_ω somewhat below the isospin prediction $a_\rho/3$ as already noticed for $D^+ \to \pi^+\mu^+\mu^-$ [6]. The strong phases δ_M remain undetermined by this and introduce theoretical uncertainties.

The situation in the $D^0 \to K^+K^- l^+ l^-$ channel is different as the obvious resonance, the ϕ, is not produced through a significant form-factor-type contribution in D^0 decays. The small $u\bar{u}$ admixture in the ϕ should give approximately few percent of the corresponding $\rho \to \pi\pi$ amplitude. Similarly, lowest lying mesons with larger $u\bar{u}$ content, $f_2(1270)$, $a_2(1320)$, decay with about 5% branching ratio to $K\bar{K}$, which again is a correction. The dominant contribution is expected to originate from annihilation topologies $D^0 \to \phi(\to K^+K^-)\gamma^*$, recently discussed in [10] for $D \to \rho l^+ l^-$ decays within QCDF. Here we continue following a phenomenological approach, as in [12], based on factorization and vector meson dominance, and use

$$\langle \gamma^*(q)\phi(p)|C_1 Q_1^{(s)} + C_2 Q_2^{(s)}|D^0(p_D)\rangle \sim C_9^{\mathrm{R}}|_{a_\phi=0} \cdot \langle V(q)|\bar{u}\gamma^\mu P_L c|D^0(p_D)\rangle \langle \phi(p)|\bar{s}\gamma_\mu s|0\rangle, \tag{32}$$

where $V = \rho^0$, ω, and we neglect differences between the $D \to \rho^0$ and $D \to \omega$ form factors. The corresponding amplitude in $D \to \pi^+\pi^- l^+ l^-$ decays, that is, when the ρ^0 which decays to $\pi^+\pi^-$ is created at the weak vertex rather than through a form factor, is effectively included in our prescription with resonance parameters fixed by data—allowing for the extra amplitude would merely result in refitting $a_\phi^{\pi\pi}$ and $a_\rho^{\pi\pi}$.[4] Specifically, for $D^0 \to K^+K^- l^+ l^-$ decays we use C_9^{R} as in (26) with $a_\phi = 0$, and the transversity form factors $F_{i\phi}$ given in the Appendix. The ϕ line shape is parametrized by a Breit-Wigner distribution. To include the contribution from $\eta \to l^+ l^-$ we use

$$\langle \gamma^*(q)\phi(p)|C_1 Q_1^{(s)} + C_2 Q_2^{(s)}|D^0(p_D)\rangle \sim C_P^{\mathrm{R}}|_{a_{\eta'}=0} \cdot \langle \eta(q)|\bar{u}\gamma^\mu P_L c|D^0(p_D)\rangle \langle \phi(p)|\bar{s}\gamma_\mu s|0\rangle. \tag{33}$$

Note, the η' is kinematically forbidden. We then obtain from (29) and the zero-width approximation for the η [35]

$$a_\rho^{KK} \simeq 0.5\ \mathrm{GeV}^2, \qquad a_\eta^{KK} \simeq 0.0003\ \mathrm{GeV}^2. \tag{34}$$

In Table I branching ratio data on $D^0 \to \pi^+\pi^- l^+ l^-$ and $D^0 \to K^+K^- l^+ l^-$ decays from LHCb [17] and BESIII [18] are shown, together with our evaluation for resonant and nonresonant branching ratios, and the predictions from [12].[5] In Fig. 2 we show the differential branching ratio $d\mathcal{B}/dq^2$ for $\delta_\rho - \delta_\phi = \pi$ (red solid curve) and $\delta_\rho - \delta_\phi = 0$ (red dotted curve). The ρ/ω-ϕ interference matters in the regions around the resonances. The $\eta^{(\prime)}$ contributions are subleading. The purely nonresonant—neither q^2 nor p^2 resonances are included—SM contribution (blue band) is much smaller than the resonance-induced distributions except for very low q^2. This remains true with BSM couplings (long-dashed purple curve) as illustrated for a maximal scenario $C_9^{\mathrm{BSM}} = 1$ (9). We learn that, unlike presently in $D \to \pi\mu^+\mu^-$ decays, in the branching ratio of $D \to \pi\pi\mu^+\mu^-$ decays and with nonresonant form factors (A1) there is no room left to probe BSM physics in the high q^2 region above the ϕ. In Fig. 2 we also show the prediction by [12] (green dashed curve). The rise of the branching ratio at very low q^2 in [12] is due to the onset of bremsstrahlung, computed using an extrapolation of Low's theorem [37], an effect which will be more pronounced for electrons as lower values of q^2 can be accessed. We recall that the soft photon approximation holds for photon energies up to m_P^2/E_P [38], $P = \pi$, K, which limits its controlled use to $q^2 \lesssim 0.1\ \mathrm{GeV}^2$ in $D^0 \to K^+K^- l^+ l^-$ and to $q^2 \lesssim 0.001\ \mathrm{GeV}^2$ in $D^0 \to \pi^+\pi^- e^+e^-$ decays. As it is a small effect on the $D^0 \to P_1P_2\mu^+\mu^-$ branching ratios, and except for the difference in phase space a lepton universal one, we refrain from including this

[4]There is a subtlety here, because the two contributions have slightly different p^2 behavior from the form factors. Since these are slowly varying functions, as opposed to the Breit-Wigner resonance shapes, this is a negligible effect within the uncertainties and the purpose of this work.

[5]There is a sign error in Eq. (25) of [12]: the relative sign between the ρ and the ω contributions from isospin must be negative, as in our (26).

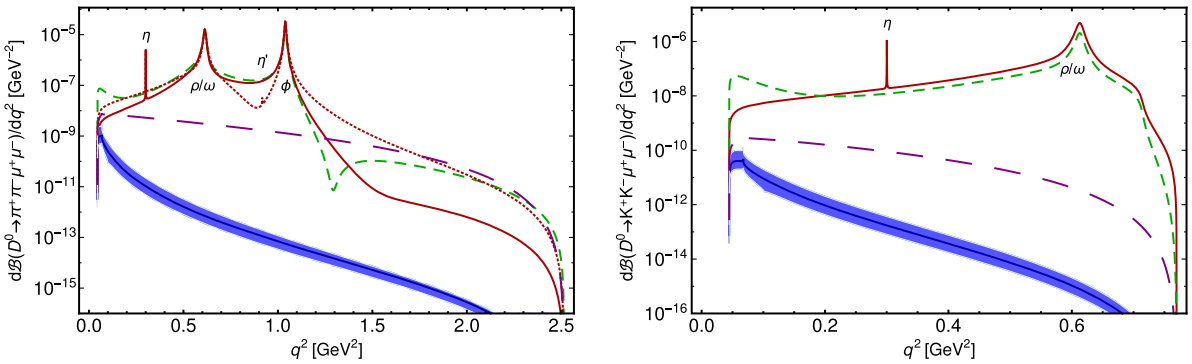

FIG. 2. The differential branching ratio $d\mathcal{B}(D^0\to\pi^+\pi^-\mu^+\mu^-)/dq^2$ (left) and $d\mathcal{B}(D^0\to K^+K^-\mu^+\mu^-)/dq^2$ (right) in the SM for central values of input. The lowest curve (blue solid) corresponds to the nonresonant prediction including uncertainties from $m_c/\sqrt{2}\le\mu\le\sqrt{2}m_c$ represented by the band. The long-dashed purple curve illustrates the impact of $C_9^{\rm BSM}=1$ on the nonresonant distribution. The resonance curves are our evaluation for $\delta_\rho-\delta_\phi=\pi$ (red solid), as from $SU(3)_F$, and $\delta_\rho-\delta_\phi=0$ (red dotted) to illustrate uncertainties related to strong phases, compared to the model [12] (green, dashed). The latter employs fixed $\delta_\rho-\delta_\phi=\pi$ and the relative sign between the ρ and the ω is as in (26), see footnote 5.

effect in our numerics. We comment on bremsstrahlung in the discussion of LNU in Sec. V C.

So far we discussed $D^0\to\pi^+\pi^-l^+l^-$ and $D^0\to K^+K^-l^+l^-$ decays. The former is special as it is the only one from (1) with a proper distribution at high q^2 above the ϕ. The latter decay is special as it is the only mode from (1) which only proceeds through the annihilation-type topology. On the other hand, the decays $D^+\to K^+\bar{K}^0l^+l^-$ are expected to have a more pronounced nonresonant contribution in p^2 as the presumably leading resonance in $K^+\bar{K}^0$ is $a_2(1320)$, with only a small branching ratio to $K\bar{K}$. The rare, semileptonic 4-body D_s decays are somewhere between the two D^0 decays, with contributions from both topologies, however, with color-enhanced annihilation at $q^2\simeq m_\phi^2$ and $m_{\eta^{(\prime)}}^2$. We stress that we employ such a phenomenological description only to obtain BSM signatures, worked out in the next section. The SM predictions, that is, specific observables being null tests, are independent of the resonance model.

V. BSM SIGNATURES

In this section we work out BSM signatures of SM null tests model-independently and in BSM scenarios with leptoquarks. For null tests related to the angular observables I_{5-9} largest effects are expected from SM-BSM interference near the resonances ρ/ω and ϕ. The dependence on the semileptonic $|\Delta c|=|\Delta u|=1$ coefficients can be taken from (21), (22).

In Secs. V A and V B we study the angular null tests $I_{5,6,7}$ and CP asymmetries, respectively. In Sec. V C we discuss ratios of dimuon to dielectron branching ratios as a probe of LNU. LFV branching ratios are worked out in Sec. V D.

A. Angular null tests $I_{5,6,7}$

We define integrated null test observables, normalized to the $D\to P_1P_2l^+l^-$ decay rate Γ,

$$\langle I_6\rangle(q^2)=\frac{1}{\Gamma}\int_{4m_\pi^2}^{(m_D-\sqrt{q^2})^2}dp^2\int_{-1}^{+1}d\cos\theta_P I_6(q^2,p^2,\cos\theta_P), \tag{35}$$

$$\langle I_{5,7}\rangle(q^2)=\frac{1}{\Gamma}\int_{4m_\pi^2}^{(m_D-\sqrt{q^2})^2}dp^2\left[\int_0^{+1}d\cos\theta_P-\int_{-1}^{0}d\cos\theta_P\right]\times I_{5,7}(q^2,p^2,\cos\theta_P). \tag{36}$$

We calculate Γ from integrating (16) over the full phase space.

We show the integrated $I_{5,6,7}$ as a function of q^2 in Fig. 3 for four BSM benchmarks $C_9^{(\prime)}=-C_{10}^{(\prime)}=0.5$ and $C_9^{(\prime)}=-C_{10}^{(\prime)}=0.5i$. The curves for $C_9^{(\prime)}=+C_{10}^{(\prime)}=0.5$ and $C_9^{(\prime)}=+C_{10}^{(\prime)}=0.5i$ can be obtained by flipping the signs of the $\langle I_{5,6,7}\rangle$, see (21), (22). The latter also explains why I_5 and I_6 have similar BSM sensitivity and why I_7 is different. As anticipated, the effects are largest where the SM contribution peaks, around the ρ/ω and the ϕ resonances. The shape between the resonances depends on their relative strong phase, shown here for $\delta_\rho-\delta_\phi=\pi$. The effect of $\delta_\rho-\delta_\phi=0$ is a reflection of the ϕ peak at the x axes. Our findings for the magnitude of $\langle I_6\rangle$ are consistent with [12].[6]

[6]Note, θ_l is defined in [12] with respect to the positively charged lepton, whereas we use the negatively charged one. It follows that $A_{\rm FB}^{[12]}=-2\langle I_6\rangle$.

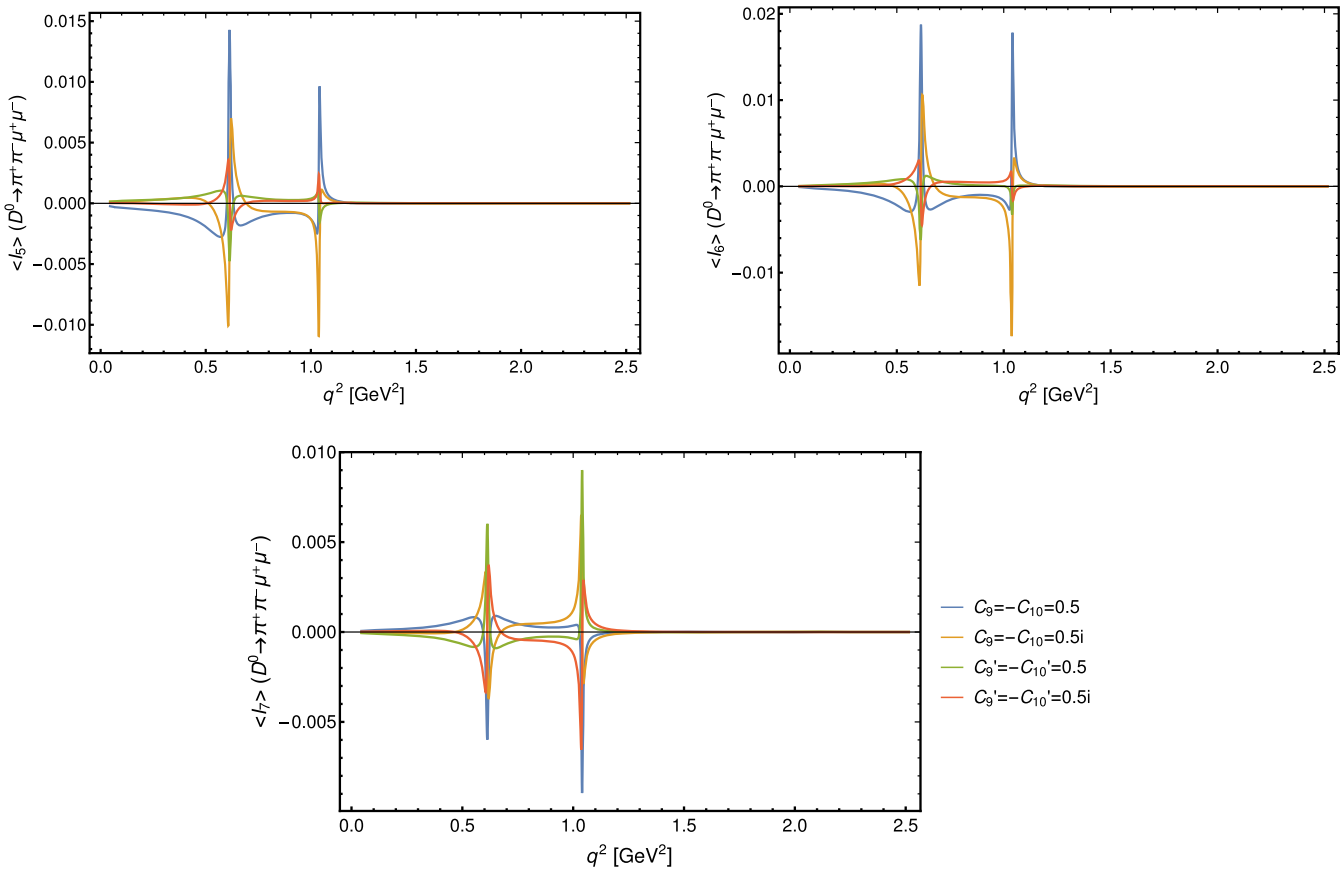

FIG. 3. Angular observables $\langle I_{5,6,7} \rangle$ integrated over p^2, see (35), (36), for $D^0 \to \pi^+\pi^-\mu^+\mu^-$ normalized to $\Gamma(D^0 \to \pi^+\pi^-\mu^+\mu^-)$ for $C_9^{(\prime)} = -C_{10}^{(\prime)} = 0.5$, $C_9^{(\prime)} = -C_{10}^{(\prime)} = 0.5i$ and relative strong phase $\delta_\rho - \delta_\phi = \pi$.

B. *CP* asymmetries without tagging

The *CP* asymmetries corresponding to the *CP*-odd angular coefficients I_k, $k = 5, 6, 8, 9$ are defined as [25]

$$A_k = 2\frac{I_k - \bar{I}_k}{\Gamma + \bar{\Gamma}} = \frac{I_k - \bar{I}_k}{\Gamma_{\rm ave}}, \tag{37}$$

where $\Gamma_{\rm ave}$ corresponds to the *CP*-averaged decay rate. The observables I_8 and I_9 can be obtained from the angular distribution (10), for instance, as follows:

$$I_8 = \frac{3\pi}{8}\left[\int_0^\pi d\phi - \int_\pi^{2\pi} d\phi\right]\left[\int_0^1 d\cos\theta_l - \int_{-1}^0 d\cos\theta_l\right] \times \frac{d^5\Gamma}{dq^2 dp^2 d\cos\theta_{P_1} d\cos\theta_l d\phi}, \tag{38}$$

$$I_9 = \frac{3\pi}{8}\left[\int_0^{\pi/2} d\phi - \int_{\pi/2}^{\pi} d\phi + \int_\pi^{3\pi/2} d\phi - \int_{3\pi/2}^{2\pi} d\phi\right] \times \frac{d^4\Gamma}{dq^2 dp^2 d\cos\theta_{P_1} d\phi}. \tag{39}$$

$I_{5,6}$ are given in (19), (17).

We define the integrated angular coefficients $\langle I_8 \rangle$ analogous to $\langle I_{5,7} \rangle$, (36), and $\langle I_9 \rangle$ analogous to $\langle I_6 \rangle$, (35). From here we obtain the integrated *CP* asymmetries $\langle A_k \rangle = (\langle I_k \rangle - \langle \bar{I}_k \rangle)/\Gamma_{ave}$. Numerical values for high q^2, $q^2_{\rm min} = (1.1\ {\rm GeV})^2$ in BSM benchmarks are given in Table II. To obtain the ranges given we varied strong phases and explicitly verified that the sign of C_9 in the first and C_9' in the second case does not matter, in agreement with (22). In the analysis of the *CP* asymmetries in (26) we effectively take into account the CKM factors $V_{cd}^* V_{ud}$ and $V_{cs}^* V_{us}$ for the ρ/ω and ϕ, respectively. The SM predictions for $\langle A_{8,9} \rangle^{\rm SM}$ at high q^2 are below the permille level, and

TABLE II. Ranges for the high q^2, $q^2_{\rm min} = (1.1\ {\rm GeV})^2$, integrated *CP* asymmetries $\langle A_i \rangle$ for $D^0 \to \pi^+\pi^-\mu^+\mu^-$ decays for different BSM benchmarks, varying strong phases.

	$C_9 = -C_{10} = \pm 0.5i$	$C_9' = -C_{10}' = \pm 0.5i$
$\langle A_5 \rangle$	$[-0.04, 0.04]$	$[-0.03, 0.03]$
$\langle A_6 \rangle$	$[-0.06, 0.05]$	$[-0.06, 0.06]$
$\langle A_8 \rangle$	$[-0.02, 0.02]$	$[-0.02, 0.02]$
$\langle A_9 \rangle$	$[-0.03, 0.03]$	$[-0.03, 0.03]$

zero for $\langle A_{5,6}\rangle^{\rm SM}$ due to the GIM mechanism, $C_{10}^{\rm SM}=0$. CP asymmetries integrated over the full q^2 region are at most permille level in BSM models, and smaller in the SM.

C. Testing lepton universality

LNU ratios in semileptonic decays [13,39,40]

$$R^D_{P_1P_2}=\frac{\int_{q^2_{\rm min}}^{q^2_{\rm max}} d\mathcal{B}/dq^2(D\to P_1P_2\mu^+\mu^-)}{\int_{q^2_{\rm min}}^{q^2_{\rm max}} d\mathcal{B}/dq^2(D\to P_1P_2e^+e^-)}, \tag{40}$$

with the same cuts in the dielectron and dimuon measurement provide yet another null test of the SM in charm as $R^D_{P_1P_2}|_{\rm SM}\simeq 1$. Phase space corrections of the order m_μ^2/m_c^2 amount to percent level effects. Electromagnetic effects are another source of nonuniversality, and expected at order $\alpha_{em}/(4\pi)\times$ logarithms, parametrically suppressed [25,28,41]. A detailed calculation is beyond the scope of this work. Within the SM we obtain for $q^2_{\rm min}=4m_\mu^2$ and $q^2_{\rm max}=(m_D-m_{P_1}-m_{P_2})^2$

$$R^{\rm DSM}_{\pi\pi}=1.00\pm\mathcal{O}(\%),\qquad R^{\rm DSM}_{KK}=1.00\pm\mathcal{O}(\%). \tag{41}$$

Beyond the SM, $R^D_{\pi\pi}$ can be modified significantly. Varying strong phases and Wilson coefficients $C^{(\prime)}_{9,10}$ one at a time within allowed ranges (9), we obtain $R^D_{\pi\pi}|_{\rm BSM}\in[0.85,0.99]$ and $R^D_{KK}|_{\rm BSM}\in[0.94,0.97]$. The latter is barely distinguishable from (41), as well as $R^D_{\pi\pi}$ and R^D_{KK} in leptoquark models, e.g., [6,40]. It is advantageous to consider the LNU ratios in bins with a smaller SM contribution to increase the BSM sensitivity. For $\pi\pi$, this is, for instance, the high q^2 region above the ϕ, $q^2_{\rm min}=(1.1\ {\rm GeV})^2$, as in [17], and with the SM prediction (41) intact. Here, in this high q^2 bin, leptoquark effects are within $R^D_{\pi\pi}|^{{\rm high}\ q^2}_{\rm LQ}\in[0.7,4.4]$, consistent with related sizable SM deviations in $D\to\pi l^+l^-$ decays at high q^2 [40]. Such sizable deviations from universality are possible for the scalar and vector $SU(2)_L$-singlet and doublet representations $S_{1,2}$, $\tilde V_{1,2}$, respectively, which escape kaon bounds because there is no coupling to quark doublets [6]. The other leptoquark representations give SM-like values for $R^D_{P_1P_2}$.

For $D^0\to K^+K^-l^+l^-$ decays we investigate possibilities to enhance the BSM sensitivity by lowering $q^2_{\rm max}$. This increases the sensitivity to lepton mass effects such that (41) does not hold anymore. We find, even when simultaneously increasing $q^2_{\rm min}$, that leptoquark-induced LNU cannot be unambiguously distinguished from the SM in the KK mode. The long-distance dominance of the branching ratio, even with BSM contributions, is also manifest from Fig. 2. For instance, below the η, for $q^2_{\rm max}=(0.525\ {\rm GeV})^2$ [17], we find that R^D_{KK} in leptoquark models is within the ballpark of the SM prediction, $R^{\rm DSM}_{KK}=0.83\pm\mathcal{O}(\%)$. On the other hand, model-independently R^D_{KK} can be suppressed relative to the SM, $R^D_{KK}|^{<\eta}_{\rm BSM}\in[0.60,0.87]$.

While data on muons [17] and electrons [18] exist for $D^0\to\pi^+\pi^-l^+l^-$ and $D^0\to K^+K^-l^+l^-$ decays, see Table I, unfortunately, this does not permit us to compute the respective clean LNU ratios (40) due to incompatible q^2 cuts employed by the two experiments. In particular, BESIII included q^2 regions not accessible with dimuons and vetoed the $\phi\to e^+e^-$ region. We recommend to give dielectron results for q^2 values above the dimuon threshold to allow for a measurement of $R^D_{P_1P_2}$ (40). Naive ratios of the branching ratio measurements [17,18] given in Table I result in lower limits,

$$\bar R^D_{\pi^+\pi^-}\gtrsim 0.1,\qquad \bar R^D_{K^+K^-}\gtrsim 0.01, \tag{42}$$

whose respective SM predictions are, due to the different q^2 cuts, subject to sizable hadronic uncertainties. Using the same cuts as in the BESIII analysis—none on the dielectron invariant mass squared except for excluding the region [0.935, 1.053] GeV [18]—we find in the model of [12] $\bar R^{\rm DSM}_{\pi^+\pi^-}\simeq 0.9$ and $\bar R^{\rm DSM}_{K^+K^-}\simeq 0.1$, about an order of magnitude away from the data. The smallness of the ratio $\bar R^{\rm DSM}_{K^+K^-}$ follows from the bremsstrahlung enhancement for electrons. A similar effect is present in the $\pi\pi$ mode, however, here it is lifted by the contribution of the ϕ in the dimuon mode. The main difference between our resonance model and [12] is, besides the use of on-peak data (27)–(29), the inclusion of bremsstrahlung effects at very low q^2, subject to systematic uncertainties as briefly discussed in Sec. IV. Lepton mass corrections in our model are small such that the main difference between electrons and muons is due to the vetoed ϕ in the denominator, $\bar R^{\rm DSM}_{\pi^+\pi^-}\sim 2$, and $\bar R^{\rm DSM}_{K^+K^-}\sim 1$. A measurement with identical cuts (40) would avoid this model dependence.

D. LFV

We work out predictions for LFV branching ratios $D^0\to\pi^+\pi^-e^\pm\mu^\mp$ and $D^0\to K^+K^-e^\pm\mu^\mp$, which vanish in the SM. Integrating the nonresonant distributions over the full q^2 range, and using the constraints discussed in Sec. II, we find model-independently and in leptoquark models, following [6],

$$\begin{aligned}\mathcal{B}(D^0\to\pi^+\pi^-e^\pm\mu^\mp)&\lesssim 10^{-7},\\ \mathcal{B}(D^0\to K^+K^-e^\pm\mu^\mp)&\lesssim 10^{-9}.\end{aligned} \tag{43}$$

VI. CONCLUSIONS

The SM angular distribution in semileptonic 4-body D-decays is considerably simpler than in B decays because of long-distance dominance in charm. The latter implies P conservation and equal chirality of the lepton currents. As a result, the angular coefficients $I_{5,6,7}$ are null tests of the SM. BSM contributions to the axial-vector coupling, $C_{10}^{(\prime)}$, can, on the other hand, induce rates at few percent level, see Fig. 3.

Rare semileptonic D^0 decays are not self-tagging and benefit from the CP asymmetries related to $I_{5,6,8,9}$, which are CP odd and do not require D tagging. Due to the smallness of $V_{cb}^* V_{ub}/(V_{cs}^* V_{us})$ corresponding CP asymmetries $A_{5,6,8,9}$ constitute null tests of the SM. BSM-induced integrated asymmetries can reach few percent, see Table II.

Ratios of branching fractions into muons and electrons (40) probe lepton universality in the up sector and complement studies with B decays. LNU tests in charm are presently not very constraining as only upper limits on branching ratios of $D \to P_1 P_2 e^+ e^-$ decays exist. We strongly encourage experimenters to provide in the future data based on the same kinematic cuts for muons and electrons, enabling more powerful SM tests.

Leptonic P invariance and suppression of SM CP violation holds in the whole (p^2, q^2)-phase space on and off-resonance peaks. Therefore, there is no particular need for cutting on $\pi\pi$ around or outside the ρ, or ll around ϕ or ρ/ω, and one can collect events from the whole phase space. Yet, experimental information on the otherwise SM-dominated branching ratios with on-resonance cuts assists tuning the hadronic model parameters. Note, near-resonance BSM signals in the angular observables I_{5-9} are larger due to enhanced interference with the SM, as exploited in [12,42] and evident in Fig. 3. On the other hand, deviations from lepton universality in the ratios (40) are enhanced in regions where the SM contribution is smaller, such as in the high q^2 region above the ϕ in $D^0 \to \pi^+\pi^- l^+ l^-$ decays, where order one BSM effects are possible. LFV branching ratios $\mathcal{B}(D^0 \to \pi^+\pi^- e^\pm \mu^\mp)$ and $\mathcal{B}(D^0 \to K^+K^- e^\pm \mu^\mp)$ can reach 10^{-7} and 10^{-9}, respectively.

ACKNOWLEDGMENTS

G. H. would like to thank the participants of the "Towards the Ultimate Precision in Flavour Physics" (TUPIFP) workshop at Warwick University for stimulating discussions. This work has been supported by the DFG Research Unit FOR 1873 "Quark Flavour Physics and Effective Field Theories" and by the BMBF under Contract No. 05H15VKKB1. We thank Giancarlo D'Ambrosio for confirmation of the sign error in Eq. (25) of [12].

APPENDIX $D \to P_1 P_2 l^+ l^-$ MATRIX ELEMENTS

1. $D \to P_1 P_2$ form factors

We employ the form factors from HHχPT [20]

$$w_\pm = \pm \frac{\hat{g} f_D}{2 f_{P_1}^2} \frac{m_D}{v \cdot p_{P_1} + \Delta},$$
$$h = \frac{\hat{g}^2 f_D}{2 f_{P_1}^2} \frac{1}{(v \cdot p_{P_1} + \Delta)(v \cdot p + \Delta)}, \tag{A1}$$

with input $\Delta = (m_{D^{*0}} - m_{D^0}) = 0.1421$ GeV, $f_D = 0.21$ GeV, $f_\pi = 0.13$ GeV, $f_K = 0.156$ GeV, $\hat{g} = 0.570 \pm 0.006$ [43], $v \cdot p_{P_1} = ((m_D^2 - q^2 + p^2) - \sqrt{\lambda(m_D^2, q^2, p^2)(1 - 4m_{P_1}^2/p^2)}\cos\theta_{P_1})/(4m_D)$ and $v \cdot p = (m_D^2 - q^2 + p^2)/(2m_D)$.

2. Resonance amplitudes

The transversity form factors for the contributions from resonances R with spin J_R read [13]

$$\mathcal{F}_0 \equiv \mathcal{F}_0(q^2, p^2, \cos\theta_{P_1}) \simeq \sum_R P^0_{J_R}(\cos\theta_{P_1}) \cdot F_{0J_R}(q^2, p^2),$$
$$\mathcal{F}_i \equiv \mathcal{F}_i(q^2, p^2, \cos\theta_{P_1}) \simeq \sum_R \frac{P^1_{J_R}(\cos\theta_{P_1})}{\sin\theta_{P_1}} \cdot F_{iJ_R}(q^2, p^2),$$
$$i = \parallel, \perp, \tag{A2}$$

where P_ℓ^m denote the associated Legendre polynomials, e.g., $P_1^0(\cos\theta_P) = \cos\theta_P$ and $P_1^1(\cos\theta_P) = -\sin\theta_P$. For vector V resonances with mass m_V and width Γ_V [13,44]

$$F_{0V} = -3N_V \frac{(m_D^2 - m_V^2 - q^2)(m_D + m_V)^2 A_1(q^2) - \lambda(m_D^2, m_V^2, q^2) A_2(q^2)}{2m_V(m_D + m_V)\sqrt{q^2}} P^V, \tag{A3}$$

$$F_{\parallel V} = -\frac{3}{\sqrt{2}} N_V \sqrt{2}(m_D + m_V) A_1(q^2) P^V, \tag{A4}$$

$$F_{\perp V} = \frac{3}{\sqrt{2}} N_V \frac{\sqrt{2\lambda(m_D^2, m_V^2, q^2)}}{m_D + m_V} V(q^2) P^V, \tag{A5}$$

with the resonance shape P^V. For the latter we employ a Breit-Wigner parametrization [45],

$$P^V(p^2) = \sqrt{\frac{m_V\Gamma_V}{\pi}}\frac{p^*}{p_0^*}\frac{1}{p^2 - m_V^2 + im_V\Gamma_V(p^2)}, \quad \text{(A6)}$$

$$\Gamma_V(p^2) = \Gamma_V\left(\frac{p^*}{p_0^*}\right)^3 \frac{m_V}{\sqrt{p^2}}\frac{1+(r_{\rm BW}p_0^*)^2}{1+(r_{\rm BW}p^*)^2}, \quad \text{(A7)}$$

$$p^* = \frac{\sqrt{\lambda(p^2, m_{P_1}^2, m_{P_2}^2)}}{2\sqrt{p^2}}, \quad p_0^* = p^*|_{p^2=m_V^2}, \quad \text{(A8)}$$

which is normalized $\int dp^2 |P^V(p^2)|^2 = 1$. For the ρ we use the Blatt-Weisskopf parameter $r_{\rm BW} = 3$ GeV^{-1} [46]. In the normalization factor

$$N_V = G_F\alpha_e\sqrt{\frac{\beta_l q^2\sqrt{\lambda(m_D^2, p^2, q^2)}}{3(4\pi)^5 m_D^3}}, \qquad \beta_l = \sqrt{1-\frac{4m_l^2}{q^2}}, \quad \text{(A9)}$$

we use the Källen function suitable for off-resonance effects, instead of $\lambda(m_D^2, m_V^2, q^2)$, and include an overall finite m_l phase space suppression. Form factors $A_{1,2}$, V are provided in [34,47,48]. Following [24] we employ the form factors by [34], parametrized as

$$F(q^2) = \frac{\tilde{F}(0)}{1-\sigma_1 q^2/m_{D^*}^2}, \quad \text{(A10)}$$

where $\tilde{F}(0) = F(0)/(1-q^2/m_{D^*}^2)$ for $F = V$ and $\tilde{F}(0) = F(0)$ for $F = A_{1,2}$. For $D \to \rho$ the parameters are given as

$$\begin{aligned} V(0) &= 0.90, & \sigma_1 &= 0.46, \\ A_1(0) &= 0.59, & \sigma_1 &= 0.50, \\ A_2(0) &= 0.49, & \sigma_1 &= 0.89. \end{aligned} \quad \text{(A11)}$$

Since the modeling of the resonances itself is accompanied by large uncertainties, we neglect the form factor uncertainties in the numerical evaluations as well as differences between $D \to \rho$ and $D \to \omega$ form factors.

For the resonance-induced $D^0 \to K^+K^-l^+l^-$ contribution we use the form factors

$$F_{0\phi} = -3N_V\frac{(m_D^2 - m_\rho^2 - p^2)(m_D+m_\rho)^2 A_1(p^2) - \lambda(m_D^2, m_\rho^2, p^2)A_2(p^2)}{2m_\rho(m_D+m_\rho)\sqrt{q^2}}P^\phi, \quad \text{(A12)}$$

$$F_{\|\phi} = -\frac{3}{\sqrt{2}}N_V\sqrt{2}(m_D+m_\rho)A_1(p^2)P^\phi, \quad \text{(A13)}$$

$$F_{\perp\phi} = \frac{3}{\sqrt{2}}N_V\frac{\sqrt{2\lambda(m_D^2, m_\rho^2, p^2)}}{m_D+m_\rho}V(p^2)P^\phi, \quad \text{(A14)}$$

where V, $A_{1,2}$ are $D \to \rho$ form factors given above. We employ a constant width (normalized) Breit-Wigner distribution for the ϕ line shape

$$P^\phi(p^2) = \sqrt{\frac{m_\phi\Gamma_\phi}{\pi}}\frac{1}{p^2 - m_\phi^2 + im_\phi\Gamma_\phi}. \quad \text{(A15)}$$

[1] G. Burdman, E. Golowich, J. L. Hewett, and S. Pakvasa, Rare charm decays in the standard model and beyond, Phys. Rev. D **66**, 014009 (2002).

[2] R. Aaij *et al.* (LHCb Collaboration), Implications of LHCb measurements and future prospects, Eur. Phys. J. C **73**, 2373 (2013).

[3] T. Aushev *et al.*, Physics at super B factory, arXiv: 1002.5012.

[4] D. M. Asner *et al.*, Physics at BES-III, Int. J. Mod. Phys. A **24**, 499 (2009).

[5] R. Aaij *et al.* (LHCb Collaboration), Search for $D_{(s)}^+$ to $\pi^+\mu^+\mu^-$ and $D_{(s)}^+$ to $\pi^-\mu^+\mu^+$ decays, Phys. Lett. B **724**, 203 (2013).

[6] S. de Boer and G. Hiller, Flavor and new physics opportunities with rare charm decays into leptons, Phys. Rev. D **93**, 074001 (2016).

[7] S. de Boer and G. Hiller, The photon polarization in radiative D decays, phenomenologically, Eur. Phys. J. C **78**, 188 (2018).

[8] S. Fajfer and S. Prelovsek, Effects of littlest Higgs model in rare D meson decays, Phys. Rev. D **73**, 054026 (2006).

[9] S. Fajfer, S. Prelovsek, and P. Singer, Resonant and nonresonant contributions to the weak $D \to Vl^+l^-$ decays, Phys. Rev. D **58**, 094038 (1998).

[10] T. Feldmann, B. Müller, and D. Seidel, $D \to \rho\ell^+\ell^-$ decays in the QCD factorization approach, J. High Energy Phys. 08 (2017) 105.

[11] I. I. Bigi and A. Paul, On *CP* asymmetries in two-, three- and four-body D decays, J. High Energy Phys. 03 (2012) 021.

[12] L. Cappiello, O. Cata, and G. D'Ambrosio, Standard model prediction and new physics tests for $D^0 \to h^+h^-\ell^+\ell^-(h=\pi,K:\ell=e,\mu)$, J. High Energy Phys. 04 (2013) 135.

[13] D. Das, G. Hiller, M. Jung, and A. Shires, The $\bar{B} \to \bar{K}\pi\ell\ell$ and $\bar{B}_s \to \bar{K}K\ell\ell$ distributions at low hadronic recoil, J. High Energy Phys. 09 (**2014**) 109.

[14] J. Brod, Y. Grossman, A. L. Kagan, and J. Zupan, A consistent picture for large penguins in $D \to \pi^+\pi^-$, K^+K^-, J. High Energy Phys. 10 (**2012**) 161.

[15] G. Hiller, M. Jung, and S. Schacht, SU(3)-flavor anatomy of nonleptonic charm decays, Phys. Rev. D **87**, 014024 (2013).

[16] S. Müller, U. Nierste, and S. Schacht, Topological amplitudes in D decays to two pseudoscalars: A global analysis with linear $SU(3)_F$ breaking, Phys. Rev. D **92**, 014004 (2015).

[17] R. Aaij *et al.* (LHCb Collaboration), Observation of D^0 Meson Decays to $\pi^+\pi^-\mu^+\mu^-$ and $K^+K^-\mu^+\mu^-$ Final States, Phys. Rev. Lett. **119**, 181805 (2017).

[18] M. Ablikim *et al.* (BESIII Collaboration), Search for the rare decays $D \to h(h')e^+e^-$, Phys. Rev. D **97**, 072015 (2018).

[19] B. Grinstein and D. Pirjol, Exclusive rare $B \to K^*\ell^+\ell^-$ decays at low recoil: Controlling the long-distance effects Phys. Rev. D **70**, 114005 (2004).

[20] C. L. Y. Lee, M. Lu, and M. B. Wise, B_{l4} and D_{l4} decay, Phys. Rev. D **46**, 5040 (1992).

[21] S. de Boer, B. Müller, and D. Seidel, Higher-order Wilson coefficients for $c \to u$ transitions in the standard model, J. High Energy Phys. 08 (**2016**) 091.

[22] S. de Boer, Two loop virtual corrections to $b \to (d,s)\ell^+\ell^-$ and $c \to u\ell^+\ell^-$ for arbitrary momentum transfer, Eur. Phys. J. C **77**, 801 (2017).

[23] S. de Boer, Probing the standard model with rare charm decays, Ph. D. thesis, Tech. U. Dortmund, 2017.

[24] S. de Boer and G. Hiller, Rare radiative charm decays within the standard model and beyond, J. High Energy Phys. 08 (2017) 091.

[25] C. Bobeth, G. Hiller, and G. Piranishvili, *CP* asymmetries in bar $B \to \bar{K}^*(\to \bar{K}\pi)\bar{\ell}\ell$ and untagged $\bar{B}_s, B_s \to \phi(\to K^+K^-)\bar{\ell}\ell$ decays at NLO, J. High Energy Phys. 07 (2008) 106.

[26] C. Bobeth, G. Hiller, and D. van Dyk, General analysis of $\bar{B} \to \bar{K}^{(*)}\ell^+\ell^-$ decays at low recoil, Phys. Rev. D **87**, 034016 (2013).

[27] C. Bobeth, P. Gambino, M. Gorbahn, and U. Haisch, Complete NNLO QCD analysis of anti-$\bar{B} \to X_s l^+ l^-$ and higher order electroweak effects, J. High Energy Phys. 04 (2004) 071.

[28] T. Huber, E. Lunghi, M. Misiak, and D. Wyler, Electromagnetic logarithms in $\bar{B} \to X_s l^+ l^-$, Nucl. Phys. **B740**, 105 (2006).

[29] C. Vacca, Measurements of charm rare decays at LHCb, arXiv:1509.02108.

[30] Y. Amhis *et al.* (HFLAV Collaboration), Averages of b-hadron, c-hadron, and τ-lepton properties as of summer 2016, Eur. Phys. J. C **77**, 895 (2017).

[31] G. Isidori and J. F. Kamenik, Shedding Light on *CP* Violation in the Charm System via $D \to V\gamma$ Decays, Phys. Rev. Lett. **109**, 171801 (2012).

[32] B. Grinstein and D. Pirjol, Factorization in $B \to K\pi l^+ l^-$ decays, Phys. Rev. D **73**, 094027 (2006).

[33] S. Faller, T. Feldmann, A. Khodjamirian, T. Mannel, and D. van Dyk, Disentangling the decay observables in $B^- \to \pi^+\pi^-\ell^-\bar{\nu}_\ell$, Phys. Rev. D **89**, 014015 (2014).

[34] D. Melikhov and B. Stech, Weak form-factors for heavy meson decays: An update, Phys. Rev. D **62**, 014006 (2000).

[35] C. Patrignani *et al.* (Particle Data Group), Review of particle physics, Chin. Phys. C **40**, 100001 (2016).

[36] L. G. Landsberg, Electromagnetic decays of light mesons, Phys. Rep. **128**, 301 (1985).

[37] F. E. Low, Scattering of light of very low frequency by systems of spin 1/2, Phys. Rev. **96**, 1428 (1954).

[38] V. Del Duca, High-energy bremsstrahlung theorems for soft photons, Nucl. Phys. **B345**, 369 (1990).

[39] G. Hiller and F. Krüger, More model-independent analysis of $b \to s$ processes, Phys. Rev. D **69**, 074020 (2004).

[40] S. Fajfer and N. Košnik, Prospects of discovering new physics in rare charm decays, Eur. Phys. J. C **75**, 567 (2015).

[41] M. Bordone, G. Isidori, and A. Pattori, On the Standard Model predictions for R_K and R_{K^*}, Eur. Phys. J. C **76**, 440 (2016).

[42] S. Fajfer and N. Košnik, Resonance catalyzed *CP* asymmetries in $D \to P\ell^+\ell^-$, Phys. Rev. D **87**, 054026 (2013).

[43] J. P. Lees *et al.* (*BABAR* Collaboration), Measurement of the $D^*(2010)^+$ Meson Width and the $D^*(2010)^+ - D^0$ Mass Difference, Phys. Rev. Lett. **111**, 111801 (2013).

[44] D. Das, G. Hiller, and M. Jung, $B \to K\pi$ll in and outside the K* window, arXiv:1506.06699.

[45] P. del Amo Sanchez *et al.* (*BABAR* Collaboration), Analysis of the $D^+ \to K^-\pi^+e^+\nu_e$ decay channel, Phys. Rev. D **83**, 072001 (2011).

[46] S. Dobbs *et al.* (CLEO Collaboration), First Measurement of the Form Factors in the Decays $D^0 \to \rho^- e^+\nu_e$ and $D^+ \to \rho^0 e^+\nu_e$, Phys. Rev. Lett. **110**, 131802 (2013).

[47] Y. L. Wu, M. Zhong, and Y. B. Zuo, $B_{(s)}$, $D_{(s)} \to \pi$, K, η, ρ, K^*, ω, ϕ transition form factors and decay rates with extraction of the CKM parameters $|V_{ub}|$, $|V_{cs}|$, $|V_{cd}|$, Int. J. Mod. Phys. A **21**, 6125 (2006).

[48] R. C. Verma, Decay constants, and form factors of s-wave and p-wave mesons in the covariant light-front quark model, J. Phys. G **39**, 025005 (2012).